Nuclear Magnetic Resonance in Solid Helium-3*

HASKELL A. REICH
IBM Watson Laboratory, New York, New York
(Received 13 August 1962)

Nuclear magnetic resonance experiments have been performed in solid He^3 at constant molar volumes in the α and β phases at various magnetic fields and temperatures by the spin-echo method. The self-diffusion coefficient D as well as the relaxation times T_1 and T_2 have been determined. D is observed to obey the Arrhenius equation as the temperature is lowered in the α phase, but at a low enough temperature it becomes temperature independent and depends only on the density. The activation energy for diffusion correlates well with that determined from specific heat measurements. At high magnetic fields T_1 and T_2 are observed to obey the Bloembergen, Purcell, and Pound relationships characteristic of relaxation caused by diffusion. At low magnetic fields, T_1 becomes temperature independent as the temperature is lowered, and is observed to depend on magnetic field as $\exp(H^2/H_0^2)$, implying that the relaxation is from Zeeman to exchange systems. Values of the exchange integral J are deduced from temperature-independent diffusion, field-dependent relaxation, and rigid-lattice values of T_2, and show fair agreement internally. No agreement can be obtained with values of J deduced from observations of departures from Curie's law, the values here reported being much smaller.

I. INTRODUCTION

SOLID He^3, because of its great simplicity, offers, perhaps, a model solid which is particularly suitable for investigation by the techniques of nuclear magnetic resonance. Three[1,2] simple, well-known, crystalline phases exist; He^3 can be obtained essentially isotopically pure, and has a nuclear spin of $\frac{1}{2}$, hence no quadrupole moment. The solid is particularly compressible, and in common with He^4, does not exist in equilibrium with the vapor. A pressure of ~ 30 atm is required to produce the solid. This solid, furthermore, has no molecular association, and He^3, along with He^4 has the lowest polarizability of any atom. The spin of $\frac{1}{2}$ has the consequence that the particles obey Fermi statistics, implies the existence of an exchange integral, and also makes possible the measurement of the self-diffusion coefficient, D.

We report here the measurement of D in the α phase, the relaxation times T_1 and T_2, in both the α and β phases, and some data on the nuclear susceptibility of the solid. We also use T_1 to determine the location of the α-β phase transition. The value of the exchange integral, J, is deduced from (a) T_2 measurements, (b) T_1 measurements as a function of magnetic field, and (c) temperature-independent D. The determination of J is carried out at a temperature range far above that at which departures from Curie's law have been observed.[3] Comparisons are made with other experimental determinations of the activation energy for diffusion, relaxation times T_1 and T_2, and determinations, both theoretical and experimental, of J by other methods. The measurements reported here were carried out at several different, constant, molar volumes from 22.48 cm^3/mole to 18.36 cm^3/mole, corresponding to pressures in the liquid at the freezing point of 69.2 and 204.5 kg/cm^2, respectively. The temperature ranged from the melting point of the solid, at most here 3.50°K, down to ~ 0.5°K.

Two different relaxation mechanisms are found to contribute to the observed spin relaxation time. The first is identified as spin-lattice relaxation caused by the self-diffusion of the He^3 atoms, and follows the relations first elucidated by Bloembergen, Purcell, and Pound (BPP).[4] The second is identified as temperature-independent Zeeman-exchange relaxation, first discussed by Kronig and Bouwkamp,[5] and later found to exist in the case of electron paramagnetic resonance in free radicals.[6] The characteristic dependence of the temperature-independent relaxation time on magnetic field can be used to determine J.

T_2 is found to become temperature independent at low enough temperatures, as shown by Van Vleck.[7] The observed value of T_2, though, is some orders of magnitude larger than calculated, due to exchange narrowing. The theory of Anderson and Weiss[8] is used also to deduce the values of J.

Since D is measured as a function of both density and temperature over a wider fractional range than in any other solid, it is informative to consider the behavior of D in the context of theories developed for more classical systems such as the alkali metals and even metallic lead.[9] It will be seen that exactly analogous

* Portions of this work have been previously reported in *Proceedings of the Second Symposium on Helium-3, 1960, Helium Three* (Ohio State University Press, Columbus, 1960), p. 63.

[1] E. R. Grilly and R. L. Mills, Ann. Phys. (New York) **8**, 1 (1959).

[2] A. F. Schuch and R. L. Mills, Phys. Rev. Letters **6**, 596 (1961).

[3] E. D. Adams, H. Meyer, and W. M. Fairbank, in *Proceedings of the Second Symposium on Helium-3, 1960, Helium Three* (Ohio State University Press, Columbus, 1960), p. 57.

[4] N. Bloembergen, E. M. Purcell, and R. V. Pound, Phys. Rev. **73**, 679 (1948), hereafter referred to as BPP.

[5] R. de L. Kronig and C. J. Bouwkamp, Physica **5**, 521 (1938).

[6] N. Bloembergen and S. Wang, Phys. Rev. **93**, 72 (1954).

[7] J. H. Van Vleck, Phys. Rev. **74**, 1168 (1948).

[8] P. W. Anderson and P. R. Weiss, Rev. Mod. Phys. **25**, 269 (1953).

[9] For a review of recent work on pressure dependence of D and applicable theories, see article by D. Lazarus, in *Advances in Solid*

behavior obtains over a wide range of densities and temperatures.

This experiment forms a continuation of previous work[10] on liquid He^3, using principally the same apparatus and techniques.

II. EXPERIMENTAL APPARATUS

The apparatus used here was substantially the same as that used by GR, except for several modifications, which are described below.

A. Sample Cell

A sample cell was here made of nylon[11] instead of the previously used cast araldite and is shown in Fig. 1. The advantages are: (1) readily machined, (2) withstands almost any predetermined design pressure (here chosen to be 335 atm), (3) withstands repeated plunging into liquid nitrogen from room temperature without cracking, (4) easily assembled; finger tight is sufficient to make a vacuum seal at room temperature, and the cell is thereafter pressure tight at 77°K to He gas at 335 atm, as measured by a mass spectrometer leak detector. It is also tight to superfluid helium. (5) Nylon is sufficiently strong so that the rf coil can be wound on the outside of the cell and still achieve a good filling factor.

This type of cell, developed in cooperation with Garwin and Low,[12] makes use of the differential thermal contraction[13] between brass and nylon to achieve a seal that tightens with decreasing temperature.

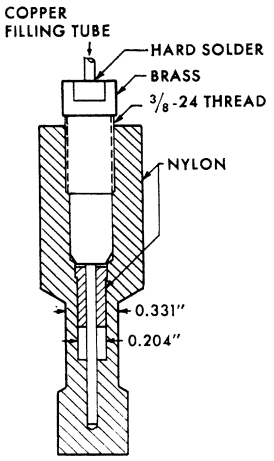

FIG. 1. Nylon-brass sample cell. Tightness is maintained at low temperatures by virtue of differential thermal contraction.

B. Electronics

In order to measure T_1 at various magnetic fields with the fixed tuned rf assembly then available, it was decided to employ the field-pulsing method. Accordingly, the magnet regulator previously used by GR was replaced by one similar to that described by Patlach,[14] and differing mainly in the number of pass transistors used. The design was such that optimum transient response for step changes in the magnetic field was realized. It took ~1 sec to decrease the field to an arbitrary predetermined value, and about 10 sec to return it from that value to the value at resonance. The procedure is described in detail in Sec. III.

It was soon found that, at low fields, the relaxation times dropped below the range of a few seconds. In view of the difficulties inherent in attempting to construct a magnet regulator with millisecond recovery times, a tuneable spin echo transmitter receiver was constructed. Since the frequency range was from ~5.2 Mc/sec to ~1.5 Mc/sec, untuned video techniques were used wherever possible. Since rapidity of tuning was also essential, an effort was made to reduce to a minimum the number of tuned circuits required.

The transmitter consisted of: (a) a low-leakage rf gate, similar to that described by Blume,[15] and differing only in that no tuned circuits were employed; (b) a General Radio 1330-A bridge oscillator, which was sufficiently stable and had low enough leakage so that no interference with the echoes resulted, and which drove the gate; (c) a 2:1 step-up pulse transformer, which coupled the gate output to the tuned circuit load whose coil surrounded the sample. The same timing chain used by GR was here used to drive the gate.

The receiver consisted of a chain of three modified Hewlett-Packard 460-A broad-band amplifiers, which had their 200-Ω input impedance matched to the sample coil by a Tektronix P-170-F cathode follower probe. The output of the amplifier chain is matched to the input of a Tektronix 535 oscilloscope by means of a tuned step-up transformer which has a gain of 10. The gain of the receiver before the oscilloscope is adjustable, and has a maximum value of 10^4, sufficient to see the thermal noise of the input circuit, and sufficient to give echo amplitudes larger than full scale on the oscilloscope. The recovery time of the receiver from the 100-V transmitter pulse was ~50 μsec.

There are thus three tuning controls, which could very conveniently be tuned in the absence of a nuclear resonance signal.

C. Gradient Shims

In order to increase the resolution for the measurement of D by the spin-echo method, it is necessary to increase the value of the magnetic field gradient to the maximum amount possible. This maximum is limited by receiver bandwidth, since as the gradient increases,

State Physics, edited by F. Seitz and D. Turnbull (Academic Press Inc., New York, 1960), Vol. 10, p. 71.

[10] R. L. Garwin and H. A. Reich, Phys. Rev. **115**, 1478 (1959), hereafter referred to as GR.

[11] Nylon grade FM 101, the du Pont Company, Wilmington, Delaware.

[12] F. J. Low and H. E. Rorschach, Phys. Rev. **120**, 1111 (1960).

[13] See Russel Scott, *Cryogenic Engineering* (D. Van Nostrand Company, Inc., Princeton, New Jersey, 1959), Chap. 10.

[14] A. M. Patlach, Electronics **33**, 66 (1960).

[15] R. J. Blume, Rev. Sci. Instr. **32**, 554 (1961).

the echo becomes narrower, and hence the spectral band occupied greater. Also, it is necessary that the transmitter pulse be short compared to the echo width.[16]

Since it was desired also to change its value on occasion, the gradient was produced by a pair of wedge-shaped shims, of 5° included angle. Use of the shims at a field of 1611 G resulted in a gradient 21 G/cm, perpendicular to the magnetic field. The gradient was determined by mapping the field with a proton resonance, and was checked by observing the shape of the echo, as in GR. Both methods gave the same result.

III. PROCEDURE

A. Blocked Capillary Method

The method by which solid He^3 of known density was produced will now be described by reference to Fig. 2, the phase diagram in the V-T plane. This diagram has been constructed from the data of Grilly and Mills[1] by subtracting the volume change on melting from the molar volume along the melting curve. Corresponding points along the melting curve on the P-T plane can be constructed by noting the temperature at which solid of a given volume melts. The temperature at which liquid of the same volume freezes is established by the pressure in the liquid. These two temperatures are then laid off on the P-T phase boundary and establish the pressure in the solid along the solid melting line. The pressure in the solid at lower temperatures is as yet unmeasured, except for some partial data along the α-β phase boundary.

To form the solid at known density, the liquid was first compressed to the desired density, while monitoring the temperature of the sample cell. A rise of several degrees due to the heat of compression and sudden introduction of hot gas established that the capillary was not blocked. The mercury level alarm, described by GR, was used to ensure that no mercury entered the capillary. The bath was then cooled to several millidegrees above the temperature corresponding to the liquid freezing point, point A. At this time a pressure of $\sim$1 mm Hg of He^4 was in the isolation space, and in the space surrounding the sample cell. He^3 liquid also filled the refrigerator, but was not pumped on. At this time, if desired, T_1 data were taken to establish a reference point for normalizing solid susceptibility. Upon ascertaining that there was no solid present inadvertently, because of errors in pressure or temperature, the temperature was lowered as rapidly as possible to some temperature where 100% solid existed, point B. The presence of a small fractional amount of solid or liquid could easily be detected because of extremely large differences in time T_1 between the solid and liquid. Due to the large latent heat of freezing, and the relatively small mass of He^3 in the capillary, and the good thermal contact between the capillary and the bath, the capillary blocked immediately upon the sudden drop in temperature, thus trapping a known molar volume in the sample cell. As long as the temperature was maintained thereafter below the melting point of the solid and the pressure maintained above the starting pressure, no slippage of material into the sample cell occurred. This was also ascertained by taking points both with decreasing and increasing temperatures, interlaced so that any change in molar volume with time would be apparent. None was ever observed. No data were taken in the mixed liquid-solid phase, as the density of the solid as well as its spatial distribution was unknown. This procedure is shown schematically in Fig. 2 as the line $ABCD$.

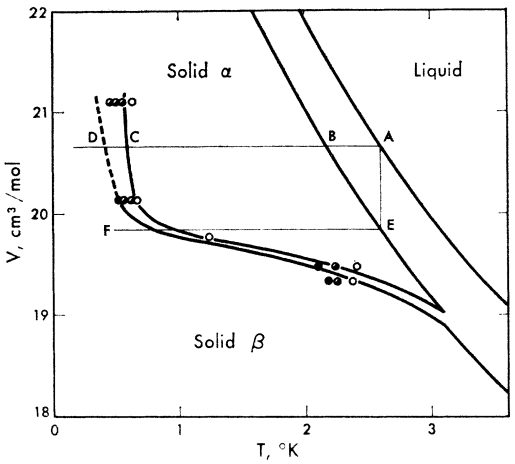

FIG. 2. Portion of the He^3 phase diagram in the V-T plane near the α-β phase transition. ○—solid α, ●—solid β, ◐—mixed solid. A-B-C-D corresponds to freezing at constant volume, A-E-F to constant pressure.

If, on the other hand, slow cooling through the liquid-solid phase boundary is allowed to occur, the molar volume of the resulting solid is represented by point E, and thereafter EF is the line followed. With intermediate rates of cooling any volume between B and E could result. However, this situation is immediately apparent since T_1 is a rapid function of molar volume, and can indeed serve to identify the volume. The molar volumes quoted are the maximum theoretical, and are estimated to be accurate to within $\sim$0.1%. Those places where the solid makes the transition from the α phase to the β phase can be recognized from the course of T_1 and T_2 with temperature. Points C, D in Fig. 2.

The data extend in pressure from 69.2 kg/cm² to 204.5 kg/cm², or volumes of 22.48 to 18.36 cm³/mole. The lower density limit arises from difficulty in reproducing the density due to the slow rate of cooling from the starting temperature, 1.79°K. The upper limit is one of convenience only, corresponding to a freezing point of 4.29°K.

[16] H. Y. Carr and E. M. Purcell, Phys. Rev. **94**, 630 (1954).

B. Electronic

Pulse Sequences

The pulse sequence used to determine D was here the same as that used in GR, 90-180-180.[16] This pulse sequence simultaneously determines D and T_2 through the appearance of two spin echoes, which are related as

$$h_2/h_1 = A \exp(-t/T_2) \exp[-(\gamma^2 G^2 D t^3/12)]. \quad (1)$$

Here h_1, h_2 are the echo heights as determined from a photograph; t, the time between the echoes; γ, the gyromagnetic ratio; G, the field gradient; T_2, the Bloch phenomenological transverse relaxation time; and D is the diffusion coefficient determined. A is a factor which describes the departure of the 180° pulse amplitude from ideality, and is left adjustable in a least-squares fit.

The determination of T_1, the Bloch longitudinal relaxation time, required several different pulse sequences, since T_1 ranged from ~ 0.03 sec to >1000 sec. The sequences used and the regions of applicability are: (a) 90-180—90-180, where the long dash refers to the variable time. This sequence is useful from the shortest times to ~ 10 sec. It requires that the sample be completely relaxed before the first 90 is applied. The equation which the data are found to obey is slightly more complicated than the simple exponential recovery, and is

$$h_2/h_1 = A - B \exp(-t/T_1),$$

where A and B are close to 1, but are left free in the least-squares fit. This allows for differences in timing between the first and second 90-180 sequence. (b) Since method (a) requires complete relaxation at the start, a method better suited for the longer relaxation times is to start from saturation. Here a sequence of 90-180 pulses is applied in rapid succession, say 10/sec for 1 sec, then a wait of variable time t, then *one* pair, 90-180. The echo grows with t as

$$h = A[1 - \exp(-t/T_1)]. \quad (2)$$

Here A is proportional to the susceptibility χ, and is later used in searching for departures from Curie's Law. Method (b) has the advantage that extremely long relaxation times may be measured from easily reproducible starting conditions, namely, saturation, and also that the measurement need not be carried past one or two time constants, thus obtaining the maximum amount of information in a given time, since the spin system need never be allowed to recover completely. It has been used to measure relaxation times up to ~ 1500 sec. Methods (c) and (d) are used for low accuracy determinations of short T_1's. Method (c) consists of a repetition of the sequence 90-180 at such a rate hat the echo amplitude is $1-e^{-1}$th of that for a long time, $\frac{2}{3}$ being an adequate approximation. For times of the order 10 msec, an even simpler scheme (d) is used. It consists of examining the amplitude of the free induction tail following a 90° pulse at a fixed time after the receiver has recovered. The spacing between 90's is then reduced until the echo amplitude is again $\frac{2}{3}$ that at long times. No statistical reduction methods were used for methods (c) and (d).

Tuning Procedure

The fixed-tuned transmitter was adjusted to produce 90° and 180° pulses by varying the plate voltage of the separate 90 and 180 generators, as discussed in GR. 180°pulses were recognized by the absence of stimulated echoes, while 90's were obtained by maximizing the echo amplitude.

The variable-frequency transmitter was adjusted by the same procedure, except that here the pulse width was varied, since the output voltage was fixed. Typical 90° and 180° pulses were 7 and 15 μsec long, respectively, and were found not to require readjustment as the frequency was changed.

The tuning procedure was best carried out after the solid was formed at some temperature just below the melting point, as here T_1 was ~ 0.1 sec. Having chosen the frequency of operation, the oscillator was set to this frequency, and the receiver was tuned by leaking in a small signal. After this, the pulser was turned on and the magnetic field was set to resonance by observing the absence of beats between the leakage signal and the echo.

C. Magnetic Field Dependence

Two different procedures were used to investigate the magnetic field dependence of T_1, corresponding to the apparatus discussed in Sec. II. The first procedure, used with the fixed tuned transmitter and receiver was as follows: Starting at H_{res}, the sample was saturated. Immediately after saturation the magnet current was switched to the new (variable) value. It was allowed to sit there a variable time t, then switched back to H_{res}. When a proton resonance field monitor indicated that H_{res} had been reached, an echo was produced and photographed. Since the time for the regulator to settle down was about 10 sec, this limited the minimum measurable value of T_1 to about 15 sec. This is the method used by Abragam and Proctor[17] and by Pershan.[18]

For shorter values of T_1 the tuneable spin echo apparatus was used, using the pulse sequences discussed in the previous section.

The region of H investigated with the two methods was allowed to overlap, as a check on consistency. The values of T_1 were identical to within experimental error, and hence are plotted without distinction as to method.

---

[17] A. Abragam and W. G. Proctor, Phys. Rev. **109**, 1441 (1958).
[18] P. S. Pershan, Phys. Rev. **117**, 109 (1960).

D. Data Reduction

The equations used to determine the values of D, T_1, and T_2 have been discussed. The equations are nonlinear, hence the "differential correction method"[19] is used, rather than to take the logarithm, and to fit straight lines, which would involve weighting the data in an unnatural way. This method assigns the same weight to each observational point, and also in the course of the calculation gives the error matrix, from which the statistical error in the calculated quantities is derived. The equation used is $\delta X=(SA_{xx}/(n-p)\Delta)^{1/2}$. Here δX is the statistical uncertainty in X, S is the sum of squares of the residuals, A_{xx} is the minor of the coefficient of X in the error matrix, n is the number of data points, usually 9 or 12, p is the number of constants determined, and Δ is the determinant of the error matrix.

E. Minimum Detectable Diffusion Coefficient

Since the echo heights are related in the 90-180-180 sequence as given in Eq. (1), the minimum detectable value of D is determined by the value of T_2, G, and the signal-to-noise ratio. G is experimentally accessible. The signal-to-noise ratio is also accessible through the expedient of working at as high a magnetic field as possible, which corresponded here to a frequency of 5.22 Mc/sec. For everything else constant, S/N varies as H^2. T_2, though is given by nature, and has its own variation with temperature. For a given value of T_2, then, how small a D can be observed? This can be seen from the following consideration: At a time $t=T_2$, the curve of h_2/h_1 vs t will have the value $1/e$ in the absence of diffusion effects. If then D is to be observable, there must be some extra damping due to the second term. Suppose the extra damping amounts to 1%. Then $1=0.01\gamma^2G^2D_{\min}T_2^3/12$ determines the minimum value of D for a given T_2. For the given value of G, 21 G/cm, and the S/N ratio, which was about 100, the minimum value of D, measured to about 50%, was $\sim10^{-8}$ cm^2/sec. It will be noted that as the temperature decreases, T_2, as well as D, gets smaller, and consequently the accuracy of determining D decreases with decreasing temperature.

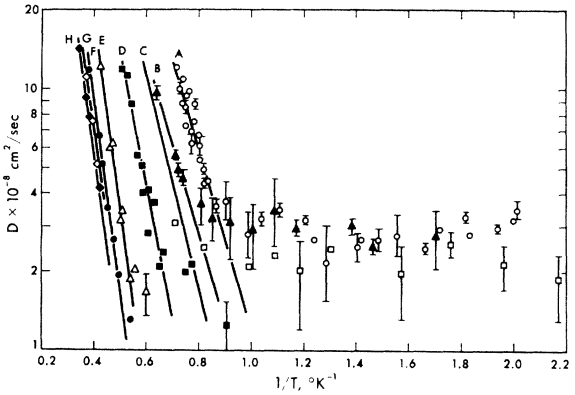

FIG. 3. Log D vs $1/T$.

[19] See, for example, K. L. Nielsen, *Methods in Numerical Analysis* (The Macmillan Company, New York, 1956).

IV. RESULTS AND DISCUSSION

Diffusion Coefficient

We present here in Fig. 3 the results of measurements of the diffusion coefficient in the α phase by the spin-echo method. Observations were made from the melting point of the solid down $\sim$0.5°K, or to the temperature at which D became too small to measure because of decreasing T_2. Table I lists the various quantities derived from Fig. 3, as well as the corresponding quantities derived from relaxation time measurements in the β phase. We note here several qualitative observations regarding the data:

TABLE I. Activation energy for diffusion and other derived data as a function of molar volume in solid He^3.

V_m (cm^3/mole)	Notes	W (°K)	D_0 (cm^2/sec) $\times10^{-5}$	D_{melt} (cm^2/sec) $\times10^{-5}$	$T_{2\,\text{rigid}}$ (msec)
22.48	All data[a]	7.82 ±0.72	3.1 ±2.0	12.4	80
	One run	8.06 ±0.25	4.0 ±0.7		
	One run +2 pts	6.69 ±0.67	1.4 ±50%		
22.05	4 pts	7.78 ±0.27	1.4 ±20%	10.2	62
21.70	All data	9.13 ±0.67	2.7 ±60%	13.4	45
21.10	[b]	11.7 ±1.2	4.8 ±70%	12.5	29
20.12		13.6	4.3	17	16
		13.8 ±0.1			
19.75		16.5 ±1.2	7 ±40%	14	<16
19.47		17.5 ±0.6	7 ±3	15	[d]
19.32	4 pts	16.9 ±1.1	5 ±2	15	[d]
	β phase, only T_1 and T_2 are observed				
20.12	[a]				15
19.47	2 pts[a]	26.0			7.5
19.32	2 pts[a]	22.4			8.2
18.82		34.1 ±0.4			3.5
18.52		38.0 ±1.0			2.6
18.36		37 ±0.4			2.0

[a] See discussion in text.
[b] At this and smaller molar volumes, the α-β phase transition is crossed.
[c] From Goodkind and Fairbank T_1, see reference 29 in text.
[d] At these molar volumes T_2 has not yet approached a constant value before the α-β transition occurs.

(a) At "high"temperatures, i.e., near the melting point, D appears to obey an Arrhenius equation of the form $D=D_0\exp(-W/kT)$.

(b) At sufficiently low temperatures, D becomes constant, independent of temperature, and depends only on density. This type of behavior has been postulated previously only for the case of rotational tunneling of certain organic molecules.[20]

(c) The value of D_{melt} is, within the accuracy of the experiment, constant and independent of temperature. Rice *et al.* have made a dynamical theory of diffusion in crystals, one of the results of which is that in the limit of low pressures there exists a law of corresponding

[20] E. O. Stejskal and H. S. Gutowsky, J. Chem. Phys. **28**, 388 (1957).

states of the form $\ln D \propto T_m/T$, which accounts for this observation.[21]

(d) W, the activation energy for diffusion, increases approximately linearly with increasing density and melting temperature. See Figs. 4 and 5.

(e) The value of D_0, the intercept at infinite temperature, is a constant, with the value $D_0 \approx 3\times10^{-5}$ cm²/sec, which is approximately the value of D in the liquid along the melting line.

Since the Arrhenius equation is apparently obeyed, if over a limited region, we may analyze the curves of Fig. 3 by the method of least squares to derive best values of the constants D_0 and W. The result of such a computation is shown in Table I. In evaluating the statistical errors here, the contribution to χ^2 from the error in each individual point has been neglected, as this is small compared to the contribution due to departure from a straight line. The data points from all

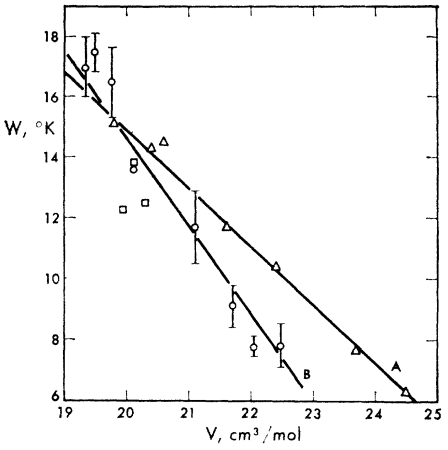

FIG. 4. Activation energy for diffusion W vs molar volume. Curve A—Swenson-Heltemes[22], Curve B—This work. The boxes give the points of Goodkind and Fairbank.[29]

available runs have been included for each reduction. There was a slight nonreproducibility of density from run to run, which condition is most difficult at the highest molar volume and there amounted to ~0.5%. At smaller molar volumes this error became negligible, but here another source of error limited the accuracy of determination of W, in that the temperature range over which the α phase exists is sharply reduced, and hence there are fewer points.

At the highest volume the curvature at the bottom makes uncertain exactly where to cut off the data. The results of a one run reduction are given, and the effect of including two points at the lower temperature are also apparent. The increased error due to combining runs is seen to be of the order of the uncertainty of W from separate runs. The adopted value in each case is

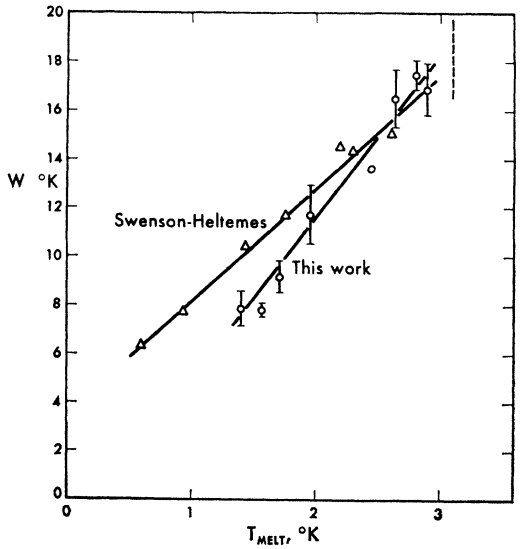

FIG. 5. Activation energy for diffusion W vs melting temperature.

the result of including all data in each run, and is the first one given.

In the β phase, the value of W is deduced from T_1 measurements. Since at the lower molar volumes, the transition occurred at rather low temperatures, there are in some cases only two data points available from which W may be determined. These are noted.

On Fig. 4 we have also plotted the activation energy for the formation of vacancies, as determined by specific-heat measurements,[22] also at constant volume. It is to be noted that there is some discrepancy between the two sets of measurements, which tends to vanish at the highest density, with W as determined from D *smaller* than W as determined from the excess contribution to specific heat. The molar volumes quoted in Table I are the largest theoretically available ones,[1] and hence if a systematic error existed in our molar volumes, the discrepancy would be worse. We, therefore, regard the discrepancy as physically real, and attempt to explain it in terms of mechanisms of diffusion developed for metals.

It was not until observation of marker movements (Kirkendall effect), and excess contributions to expansion coefficients and specific heats that the mechanism for diffusion in metallic crystals was uniquely established as due to vacancies and interstitials.[9] The measured activation energy, W, is generally thought of as consisting of the sum of two parts: $W=E_v+E_m$, where E_v is the energy required to form a vacancy, and E_m is the additional energy required to move the vacancy (or interstitial) across some internal potential barrier.[23] The excess specific heat near the melting point

[21] R. A. Hultsch and R. G. Barnes, Phys. Rev. **125**, 1832 (1962).

[22] E. C. Heltemes and C. A. Swenson, Phys. Rev. Letters **7**, 363 (1961).

[23] G. J. Dienes, Phys. Rev. **89**, 1851 (1953).

of AgBr has been analyzed[24] as due to the energy E^a. The agreement with the number of vacancies deduced from electrical measurements of mobility was considered good. Heltemes and Swenson have measured E_v as a function of density, and a measurement of D should give E_v+E_m, both positive quantities. Since W was observed here to be even smaller than E_v, we conclude that there is another mechanism of diffusion operating in parallel with the usual vacancy mechanism, which gives rise to a lower activation energy. From observation (b) we also conclude that a vacancy mechanism alone is insufficient to explain D, because the number of vacancies must decrease exponentially with decreasing temperature, assuming they obey Boltzmann statistics. The most probable remaining mechanism then, is the one identified[25,26] as "ring of two" or direct exchange, or translational tunneling.

One cannot carry the analogy between the behavior of solid He^3 and solid metals too far: He^3 is a solid where quantum effects are very large. In particular, the amplitude of zero-point motion has been estimated[27,28] to be about 0.3 a, where a is the interatomic spacing. Since the exchange frequency which results from this large overlap can be thought of as the time required for two atoms to change places, we may attempt to identify the characteristic jump frequency for diffusive motion with the exchange frequency. We do this for the molar volume 22.48 cm^3/mole, where we may expect the largest effects due to exchange. Using $D=\langle r^2\rangle/6\tau_c$, $D=3\times10^{-8}$ cm^2/sec, and $r=3.64\times10^{-8}$ cm, we obtain $J=\tau_c^{-1}=1.36\times10^8$ cps, or $J=6.52\times10^{-3}$ °K, which is close to the value predicted in references 27 and 28. This frequency may be compared to the frequency of zero-point motion, obtained from the Debye frequency appropriate to a θ of 21.1°K,[22] here a factor 3200 larger. We are thus led to characterize the solid as one in which an atom is not well localized, undergoes large amplitude vibrations, and once every 3200 vibrations (on the average) changes places with a neighbor. Since the atoms are here labeled by their spins, it is physically indistinguishable if two atoms actually change places, or if their spins mutually exchange, in defining diffusive jumps. We note further that this mechanism would be temperature independent, as is observed.

As the density is increased, the temperature-independent part of D gets smaller, which implies that the exchange integral is also getting smaller. Unfortunately, this part of D soon gets below the limit of observability, due to decrease of T_2 with increasing density. Presumably, if a larger gradient could be used, the temperature-independent part of D would then be observable at higher densities.

As the density is increased then, the exchange contribution to the diffusion coefficient gets smaller, and hence the observed activation energy approaches more closely the value deduced from specific-heat measurements, as shown in Figs. 4 and 5.

Value of D_0

Theoretical estimates have been made of the value of D_0, the "frequency factor"[23] in the Arrhenius equation. Since these arguments rely on statistical thermodynamics, they do not depend on any particular metallic property of the substance, and may be applied to solid He^3. Dienes writes for D,

$$D=[\gamma\nu\lambda^2e^{\Delta S/R}]e^{-(E_v+E_m)/T},$$

where the expression in the brackets is D_0, and where $\gamma=\frac{4}{3}$ for He^3 in the α phase (bcc), $\nu=$ the vibrational frequency of an atom, here taken to be the Debye frequency, λ the jump distance, and ΔS the entropy of activation. E_v and E_m are defined above. ΔS is composed of the sum of three parts: (1) A contribution due to thermal expansion of the lattice; (2) a contribution due to altered vibrational frequencies around a vacancy; and (3) the contribution due to altered frequencies around a saddle point. Since the measurements here are taken at constant density, contribution (1) vanishes, and we need consider only (2) and (3). Choosing the constants as above, $\nu_D=k\theta/h=4.4\times10^{11}$ cps, $r^2=1.33\times10^{-15}$ cm^2, and $D_0=4\times10^{-5}$ cm^2/sec, we obtain $e^{\Delta S/R}=0.051$ or $\Delta S=-5.9$ eu. The theoretical calculated value of ΔS_3 is approximately -9 to -10 eu for most lattices with Grüneisen's constant $\gamma=2.24$, so we see that the value of ΔS_2 is $\sim+3$ or 4 eu, consistent with the calculation of Mott and Gurney quoted in reference 23.

Previous measurements of pressure variation of D have been mainly concerned with determining the pressure dependence of W.[21] In these the experimental method was carefully arranged so that any possible variation in D_0 was not observed. Theories of D_0, on the other hand, have built into them the possibility of observing pressure variations.

Figure 4 has plotted on it also the results of Goodkind and Fairbank[29] on solid He^3 obtained by means of free-precession techniques. They determined the activation energy by observing T_1 at a frequency of 30.4 Mc/sec. Since Goodkind and Fairbank took data as a function of pressure, they were able to evaluate the volume of activation, knowing $\partial W/\partial P$. Since this experiment was at constant volume, such a comparison is not possible, in the absence of knowledge of the compressibility and thermal expansion coefficient of the solid.

[24] R. W. Christy and A. W. Lawson, J. Chem. Phys. **19**, 517 (1951).
[25] H. B. Huntington and F. Seitz, Phys. Rev. **61**, 315 (1942).
[26] C. Zener, Acta Cryst. **3**, 346 (1960).
[27] N. Bernardes and H. Primakoff, Phys. Rev. **119**, 968 (1960).
[28] E. M. Saunders, Phys. Rev. **126**, 1724 (1962).
[29] J. M. Goodkind and W. F. Fairbank, Phys. Rev. Letters 4, 458 (1960) and reference 3, p. 52, hereafter referred to as GF.

Relaxation Time T_1

The spin relaxation time T_1 is shown in Fig. 6, plotted vs T^{-1} for various values of molar volume in both the α and β phases. The data here were again taken at $H_0=1611$ G. From the observation that T_1 decays were always purely exponential, we conclude that spin diffusion and relaxation by paramagnetic impurities were not important.[30]

It was further noted that T_1 was independent of the gradient used ($\sim$21 and 1 G/cm). Hence no distinction is made in plotting. In the course of measuring T_1 an attempt was also made to detect any possible shifts in the frequency of resonance due for example to bulk magnetization, or other possible cooperative effects. Since the magnet, at best, did not have a very small gradient, the accuracy was limited to $\sim 1/10^4$. No shifts of resonant frequency this large were detected, using a proton resonance as the field monitor.

Observations concerning T_1 are as follows:

(1) In the α phase, near the melting point T_1 shows behavior typical of relaxation to the lattice caused by diffusion. As the temperature is lowered T_1 decreases, sometimes going through a minimum, depending on the density. The slope is expected to be asymptotic to the activation energy for diffusion. The actual slopes in the α phase are slightly less, because the solid melts, in most cases, before a straight line is found. The β phase is always well on the long correlation time side of the curve, so that a straight line is found from which the activation energies are deduced.

(2) For some values of the density in the α and β phases T_1 becomes constant as the temperature is lowered down to the lowest temperature of 0.5°K. This behavior is identified with a competing relaxation mechanism, Zeeman exchange, and here T_1 depends on the value of H_0.

(3) For some densities there is a discontinuous jump in T_1 and the activation energy, which serve to locate the α-β phase transition. Indeed, in some narrow temperature range mixtures of α and β can be identified by the appearance of nonexponential recovery. These can be analyzed as the sum of two exponentials to show the relative fractions of α and β, as well as the respective T_1's. The data are not used, however, because a coexisting mixture of α and β has different density for each component, and hence cannot be plotted on the same constant density curve. There is, at most densities, an accompanying discontinuous change in T_2. Further discussion of the α-β phase transition is found below.

(4) At the melting point it is observed that at the frequency 5.224 Mc/sec, the α phase is always on the short correlation time side and the β phase on the long correlation time side of the relaxation time curve.

(5) We further note that T_1 in the α phase near the melting point shows a monotonic decrease as the density is increased, and can serve to identify which of two closely spaced runs has the higher density. This observation is used in conjunction with the runs at 19.47 and 19.32 cm^3/mole.

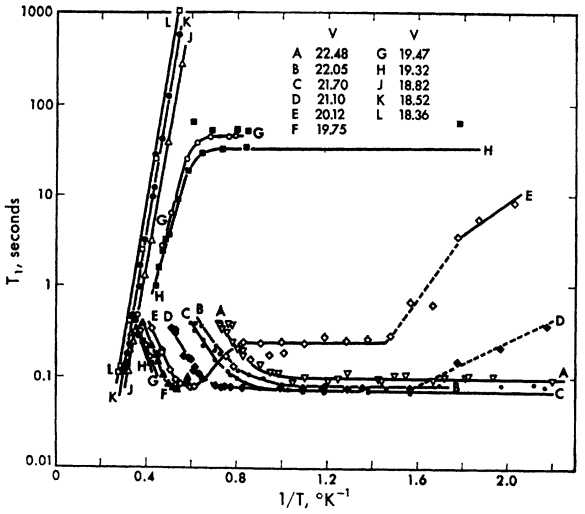

FIG. 6. Relaxation time T_1 vs $1/T$, showing transition to β phase in curves D, E, G, and H.

The theory of BPP, first used to explain spin-lattice relaxation caused by self-diffusion in a liquid was later modified by Torrey[31] to account for relaxation in solids where there is a fixed jump distance to nearest-neighbor sites. Holcomb and Norberg[32] have investigated relaxation in alkali metals, and have shown that the partial contribution to the relaxation rate caused by the independently measured diffusion coefficient obeys Torrey's equation. In our case there are no conduction electrons, so matters are simpler.

Torrey's Eq. (86) predicts the variation of T_1 with temperature and magnetic field through

$$T_1^{-1}=(8\pi/5)\gamma^4\hbar^2 I(I+1)(n/k^3 l^3\omega)\psi(k,y)=K_1\psi. \quad (3)$$

Here T_1 is the relaxation time; n, the number density; $k=0.76293$, a constant which depends on the lattice type; l is the nearest-neighbor (jump) distance; and ω is the resonant frequency. $\psi(k,y)$ is a tabulated function which contains the variation due to temperature through $y=\frac{1}{2}\omega\tau_c$. The correlation time τ_c is to be identified with the mean time between jumps, and varies with T as $\tau_c=\tau_0\exp(W/T)$. The function ψ has a maximum value, corresponding to optimum correlation time for relaxation at $y=0.5922$, where $\psi_{\max}=0.28955$. We see that the only unknown constant is τ_0.

Torrey's equation should be most useful in the vicinity of the minimum, where T_1 is most sensitive to the exact nature of the diffusion process. Far from the

[30] W. E. Blumberg, Phys. Rev. **119**, 79 (1960).

[31] H. C. Torrey, Phys. Rev. **92**, 962 (1953); **96**, 690 (1954).

[32] D. F. Holcomb and R. E. Norberg, Phys. Rev. **98**, 1074 (1955).

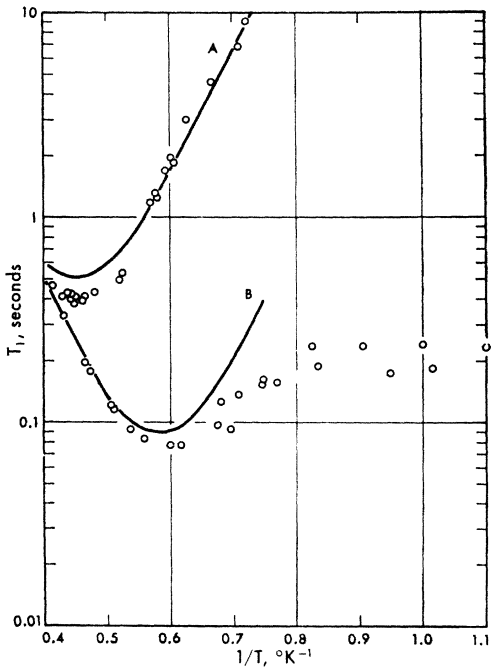

FIG. 7. Relaxation time T_1 vs $1/T$ for $V=20.12$ cm^3/mole, at 30.4 Mc/sec (Curve A) and 5.224 Mc/sec (Curve B). The curves are calculated using BPP theory, as explained in the text.

minimum, the exact shape does not depend on the details of the process, and Torrey's equation assumes the same asymptotic form as the BPP theory.

Since Torrey's theory also contains the frequency dependence, we seek to compare the theory with experiments for which data are available at differing frequencies. Fortunately, Goodkind and Fairbank[29] have presented a relaxation curve at a volume very close to one at which we worked, $V=20.12$ cm^3/mole. The data are shown in Fig. 7. Since the GF data have the qualitative appearance we seek, we attempt to fit the Torrey curve to their data first. Since the activation energy of 13.8°K is well determined, we regard it as a fixed constant, and we have available at our disposal only the value of τ_0, which is chosen to make the minimum in T_1 occur at $T^{-1}=0.455$°K^{-1}. We then calculate K_1, and obtain its theoretical value, 5.88, compared to an observed value of 8.63. We, therefore, choose to regard this constant also as having an adjustable value, to be determined from the experimental data. We will, however, retain the dependence on ω in the form given. If, then, the Torrey calculation is carried out, it is found that the asymptotic value at long correlation times (low temperatures) has the appropriate slope, but is too small in absolute value by $\sim 40\%$, and the corresponding curve obtained by inserting the value of ω appropriate for this experiment shows a correspondingly poor fit. If attempts are made to fit the Torrey curve to the straight line portion by adjusting K_1 equally bad agreement is obtained. The GF data appear to have a sharper minimum than that expected from Eq. (3).

We therefore return to the BPP formulation of relaxation due to diffusion, as perhaps the lattice structure of solid He^3 is "loose" enough so that a theory developed for liquids may be applicable.

The BPP equation for relaxation has the form

$$\frac{1}{T_1}=\frac{K_2}{\omega}\left(\frac{x}{1+x^2}+\frac{2x}{1+(2x)^2}\right), \tag{4}$$

where $x=\omega\tau$ and τ varies with temperature as before. This expression has a maximum at $x=\sqrt{2}/2$. If we now choose K_2 and τ_0 so that the curve passes through the same minimum point, the low-temperature asymptote then lies $\sim 25\%$ below the experimental data. We see that the agreement is better but still falls wide of the data. We may choose a different method of fitting the curve, namely, fix the temperature of the minimum to agree with the data and fix the asymptotic value to pass through the data points by adjusting K_2. The value of $T_{1\min}$ will then be determined. This is the procedure used to construct curves A and B on Fig. 7. The values of the parameters determined by this method are: $K_2=6.35\times 10^8$ sec^{-2}; $W=13.8$°K; and $\tau_0=6.94\times 10^{-12}$ sec. We may compare the value of τ_0 thus derived with the value of τ_0 derived from diffusion, using $D=\langle r^2\rangle/6\tau_c$, which for this density is $\tau_0=5.32\times 10^{-12}$ sec. The agreement is considered satisfactory in view of the uncertainties caused by the possible two mechanisms of diffusion. It is seen that the GF data appear to have a sharper minimum even than BPP theory would predict. Incidentally, if we consider only the data near the minimum, and disregard the asymptotic value, there is no experimental basis for distinguishing between the BPP and Torrey theories—both fit equally well.

Although it has been shown[33,34] that the theory of BPP is in error, in that the second term of Eq. (4) should be twice as large, and that Torrey's theory suffers from the same error in deriving Eq. (3), calculation shows that the shape of the curves derived from the two theories are independent of the exact coefficient used for the double frequency term, to better than 1%. The only difference which appears is that the value of K_2 is changed by about 30%, in such a way as to be in closer agreement with the experimental value. The position of the minimum is shifted slightly, but insignificantly.

The value of $T_{1\min}$ in this experiment, lower than predicted from Eqs. (3) and (4), the fact that it occurs at a lower temperature, and the temperature independence of T_1, all are caused by the added relaxation due to exchange which becomes operative at low enough

[33] A. Abragam, *The Principles of Nuclear Magnetism* (Oxford University Press, New York, 1961), pp. 300 and 462.

[34] R. Kubo and K. Tomita, J. Phys. Soc. Japan 9, 888 (1954).

temperatures. However, qualitative agreement at high temperatures obtains with BPP theory.

Field Dependence of T_1

In order to explain the qualitative disagreement between GF and these T_1 measurements, it is necessary to discuss the spin Hamiltonian appropriate to solid He^3, which we take to be in the form[6,7]

$$\mathcal{H}=\mathcal{H}_0+\mathcal{H}_{ex}+\mathcal{H}_{dip}. \tag{5}$$

Here $\mathcal{H}_0$ is the Zeeman energy in the external field

$$\mathcal{H}_0=\gamma H\sum_j \mathbf{I}\cdot z_j, \tag{6}$$

and the exchange and dipole energy terms are given by

$$\mathcal{H}_{ex}=\sum_{k>i} J_{ik}\mathbf{I}_i\cdot\mathbf{I}_k, \tag{7}$$

$$\mathcal{H}_{dip}=\gamma^2\sum_{k>i}\left[r_{ik}^{-3}\mathbf{I}_i\cdot\mathbf{I}_k-3r_{ik}^{-5}(\mathbf{r}_{ik}\cdot\mathbf{I}_i)(\mathbf{r}_{ik}\cdot\mathbf{I}_k)\right., \tag{8}$$

which differs from the Hamiltonian customarily used to analyze paramagnetic resonance experiments only in that the spins here are nuclear rather than electron spins.

Since the magnetic moments are $\sim 10^{-3}$ as large for nuclei than for electrons, we may expect that at easily attainable fields,

$$\mathcal{H}_{ex}\approx\mathcal{H}_0. \tag{9}$$

And if the exchange is at all large, we may also expect that

$$\mathcal{H}_{ex}\gg\mathcal{H}_{dip}. \tag{10}$$

Since $\mathcal{H}_{ex}$ commutes with $\mathcal{H}_0$, and $\mathcal{H}_{dip}$ weakly couples the two, we may assign separate spin temperatures to the Zeeman and exchange systems in the region where $T_1\gg T_2$. The total system may then be described by the diagram of Fig. 8.

In the spin-echo experiment, the measured quantity, T_1, is characteristic of the recovery of M_z from saturation, which can occur through two processes: (1) Zeeman-lattice relaxation, characterized by a time T_{ZL}, and (2) Zeeman-exchange relaxation, characterized by a time T_{ZE}. The Zeeman-lattice relaxation is temperature dependent, through the coupling introduced by the random fluctuations of $\mathbf{r}$ due to diffusive motion, and is given in Eq. (4). T_{ZL} varies asymptotically for large H as H^2. The Zeeman-exchange relaxation does not depend on temperature, because the coupling arises from that part of the Hamiltonian which commutes with $\mathcal{H}_0+\mathcal{H}_{ex}$. T_{ZE} varies with H as

$$T_{ZE}=T_2\exp(H^2/2H_l^2), \tag{11}$$

where H_l is some "local" field.[34]

It might be assumed that the observed T_1 is related to T_{ZE} and T_{ZL} through an equation characteristic of independent rate processes,

$$1/T_1=1/T_{ZE}+1/T_{ZL}.$$

But such an equation would predict a temperature-independent relaxation at both high and low temperatures, contrary to the observed shape shown in Fig. 7. In addition, the detailed shape of the T_1 vs H^2 curve shown in Fig. 9 in the region where both terms have comparable magnitudes is not reproduced.

The mechanism by which the Zeeman energy relaxes toward the exchange bath was first given on a classical basis by Kronig and Bouwkamp,[5] who first predicted the variation $\exp(H^2/H_l^2)$. This result was obtained by considering the scalar part of the dipole interaction, and since the exchange interaction is also a scalar, the effects are inseparable. The local field may thus be considered to arise from two sources, dipole-dipole and exchange, where it is anticipated that the exchange field

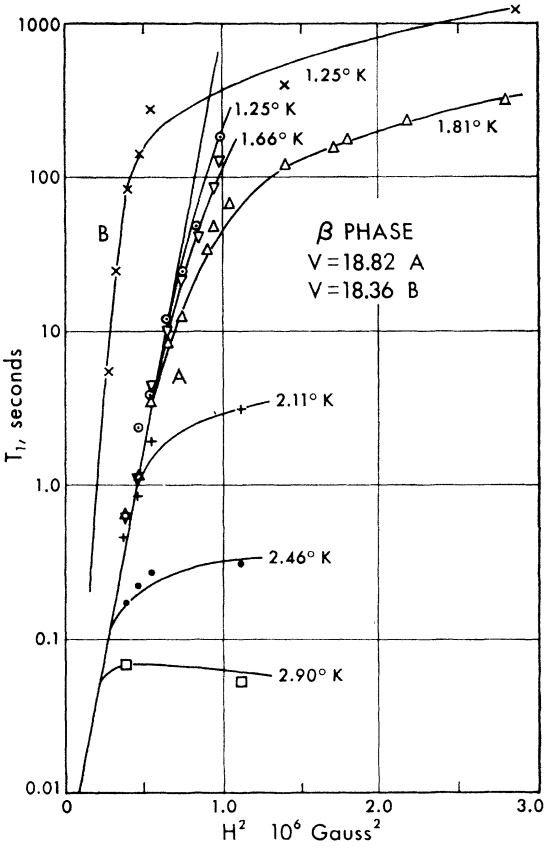

FIG. 9. Log T_1 vs H^2, at various temperatures. The straight line portion is temperature independent. At high fields, the curves depend on H as H^2.

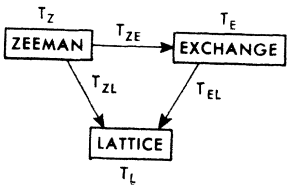

FIG. 8. Schematic showing the various relaxation times and bath temperatures.

will be very much larger than the dipole field of a few gauss.

The theory was later extended on a quantum-mechanical basis by Kubo and Tomita[34] and Yokota.[35] These theories were used by Bloembergen and Wang[6,36] to explain the anomalous linewidths found in paramagnetic salts.

In Fig. 9 we plot the observed T_1 vs H^2, for several different values of the temperature, for the constant volumes of 18.82 and 18.36 cm³/mole, entirely within the β phase. The region in which the relaxation time T_1 is temperature independent is clearly apparent, as is the region where $T_1 \propto H^2$ and depends on temperature through Eq. (4). The slope of the straight line in Fig. 9 may be used to deduce the value of H_l, which is to be identified with a fictitious exchange magnetic field through $H_{ex}=J/\gamma$. The values of the exchange field are thus determined to be 208 and 142 G, corresponding respectively to the molar volumes above. The smallest field at which data were taken was ~500 G; these data confirm the expectation of Eq. (9). The corresponding exchange frequencies are 0.68 Mc/sec and 0.46 Mc/sec, which are somewhat smaller than the values deduced in Table II. It is also seen that the intercept at $H=0$ corresponds fairly well with the observed value of T_2.

Following the methods of reference 34, Hartmann[37] has derived an exact expression for the relaxation rate $1/T_1$ valid for any combination of resonant frequency, diffusive jump time, and exchange frequency. This derivation treats the diffusion-determined properties in the same manner as BPP, and contains the specific properties of the lattice only in the coefficient of the double frequency term.

Hartmann finds (tentatively)

$$1/T_1=K_3\,\mathrm{Re}\{W(x+iy)+2\alpha W(2\alpha x+iy)\}, \quad (12)$$

where $z=x+iy$ and

$$W(z)=e^{-z^2}\left\{1+\frac{2i}{\sqrt{\pi}}\int_0^z e^{-t^2}dt\right\}, \quad (13)$$

and where $x=\omega/\sqrt{2}\omega_e$ and $y=1/\sqrt{2}\omega_e\tau$. The constant α depends on the lattice type, and for a bcc lattice Hartmann finds the value 0.837. Equation (12) has the proper asymptotic behavior in the regions where either exchange or diffusion predominate in causing relaxation. The ratio of the relaxation time at the minimum to temperature independent relaxation time serves to uniquely determine the parameter x, and hence ω_e. A comparison of the curves in Hartmann's paper with our experimental data yields, for $\alpha=1$, $x=1.46$, from which we determine $J=5.1\times10^6$ cps. This value is to be compared to the value $J=7.8\times10^6$ cps for this density as derived from the rigid lattice value of T_2 (see below).

The agreement is considered satisfactory. Goodkind and Fairbank[29] have reported, for a molar volume of 20.12, that the spin relaxation time at ~0.1°K was about 2400 sec. Assuming then, that $T_1 \propto \exp(H^2/2H_l^2)$, we may calculate the temperature-independent value of T_1 expected at 30.4 Mc/sec. This value is $\sim10^6$ sec. However, from examination of Fig. 6 (Curve E) it is apparent that at 0.1°K the solid is in the β phase, and hence no comparison is possible with solid in the α phase.

We also note that the tentative hypothesis advanced previously in reference 3 (p. 63) that the temperature independent relaxation was caused by quantum tunneling, (independent of magnetic field) is erroneous.

The same effect which causes the BPP and Torrey theories to be insensitive to the exact value of the coefficient of the double-frequency term operates here, and the shape of the curves of Eq. (12) are little affected by choice of α. We have, therefore, chosen $\alpha=1$, consistent with the choice in Eq. (4). The choice of α does affect the value of x in Eq. (12), and hence the deduced value of ω_e. The difference, though, amounts to at most 10%. Equation (12) can also be used to reproduce the field-dependent curves of Fig. 9, by choosing only τ_0. The slope of the straight line portion is found to be $\omega^2/2\omega_e^2$, and hence determines ω_e simply, notwithstanding the fact that there are two terms in Eq. (12). The intercept is experimentally determined, and is thus independent of any assumptions used to derive Eq. (11). The only remaining parameter is y, which depends on the temperature in a known manner. A calculated family of curves of T_1 vs H^2 is presented in Hartmann's paper.

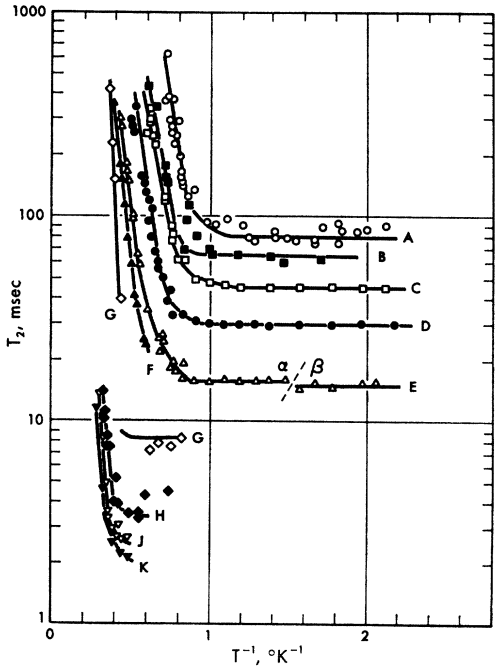

FIG. 10. Log T_2 vs $1/T$, showing the discontinuous change from α to β, and the rigid-lattice values.

[35] M. Yokota, J. Phys. Soc. Japan **10**, 762 (1955).
[36] N. Bloembergen, S. Shapiro, P. S. Pershan, and J. O. Artman, Phys. Rev. **114**, 445 (1959).
[37] S. R. Hartmann (to be published).

Another observation of interest was the fact that the T_1 relaxation curves were always accurately exponential, even in the region where $H \approx H_{ex}$, as in the β phase. This implies that the temperature of the exchange bath does not change during the relaxation process. This, in turn, may arise in two ways: Either the exchange specific heat is very high, or the exchange-lattice relaxation time T_{EL} is very short, say of order 1/10 of the shortest T_1 observed (which was ~ 0.1 sec), or less.

The specific heats of the Zeeman and exchange systems have been given[6] as

$$C_z = CH^2 T_Z^{-2}, \tag{14}$$

$$C_{ex} \approx CH_{ex}^2 T_{ex}^{-2}. \tag{15}$$

Since we operate at $H_{ex} \approx H$, we are led to conclude that T_{EL} must be very short, and indeed, since T_2 is here ~ 0.01 sec, $T_{EL} \approx T_2$, in this range of temperature and magnetic field, in accord with the predictions of reference 34.

Garwin and Landesman,[38] in extending the range of temperature downward, have discovered another, long, relaxation time, involved in the approach to equilibrium of the Zeeman system. This relaxation time can be much longer than T_{ZE} and they consequently conclude that the exchange specific heat is much larger than that given by Eq. (15). This experiment did not detect any such effects in the range of parameters investigated, although the interpretation of reference 38 is not excluded.

Relaxation Time T_2

We present the data of transverse relaxation time T_2 in Fig. 10, plotted in the same manner as the T_1 data. We do not make use of the temperature-dependent part, except for some qualitative observations. The temperature-independent part is discussed in terms of the Van Vleck second-moment theory for a rigid lattice, extended by Anderson and Weiss for the case of exchange narrowing. At high temperatures it is found that T_2 is of the exponentially activated form, as is to be expected from the BPP theory of motional narrowing. In the α phase, $T_1 = T_2$ near the melting point. But since the expression for T_2 is analytically awkward, we do not attempt to calculate T_2 in this region. It is observed though, that T_2 decays are always exponential, giving evidence for Lorentzian line shape instead of Gaussian. The relation between T_2 decays and line shape measurements has been discussed at length by Lowe and Norberg.[39]

At some low enough temperature, T_2 no longer shows the effects of motional narrowing and becomes temperature independent. In such a case, we may use the Van Vleck calculation of the second moment[7] to find the expected value of T_2.

Van Vleck gives, for a simple cubic lattice, powdered,

$$\langle \Delta\omega^2 \rangle_{av} = (3/5)\gamma^4 \hbar^2 I(I+1) \sum 1/r^6. \tag{16}$$

We assume, in view of the approximations already made in deriving this expression, that the corresponding linewidth for the case of bcc and hcp lattices may be obtained by just performing the proper lattice sum. We use, therefore, $\sum r^{-6} = 29.06\, a^{-6}$ for bcc where a is the cell edge, and $\sum r^{-6} = 14.45\, a^{-6}$ for hcp, where here a is the nearest-neighbor distance. Inserting the proper values of the constants, we obtain

$$T_2' = 2.102 \times 10^{-6} V \text{ sec bcc},$$

$$T_2' = 2.980 \times 10^{-6} V \text{ sec hcp}.$$

Here we have identified $1/T_2' = \langle \Delta\omega^2 \rangle_{av}^{1/2}$, consistent with Lorentzian line shape. V is the molar volume.

Anderson and Weiss[8] have calculated the second and fourth moments of strongly exchanged narrowed lines and, by comparing the expressions with the corresponding ones of Van Vleck, have derived

$$\omega_e^2 = (8.48/3)(J/\hbar)^2 I(I+1), \tag{17}$$

and

$$\Delta\omega = \omega_p^2/\omega_e = \langle \Delta\omega^2 \rangle_{av}/\omega_e. \tag{18}$$

Combining these, we obtain

$$J = (T_2')_{obs}/1.26(T_2')_{calc}^2 (\text{sec}^{-1}). \tag{19}$$

The observed T_2 decay consists of two parts: $(1/T_2')_{obs} = (1/T_2') + 1/T_1$. BPP have written $\frac{1}{2}T_1^{-1}$ as the amount to be subtracted from $1/T_1$ to obtain $1/T_2'$, but this holds only where the line shape is Gaussian. We use the form appropriate to Lorentzian lines.

Table II lists the value of T_2 observed, T_2' as obtained above, the rigid lattice value of T_2', and the derived value of J, in units of cps and millidegrees. T_2

TABLE II. Value of exchange integral J calculated from rigid lattice value of T_2 and theory of Anderson and Weiss (See reference 8).

V (cm³/mole)	$T_{2\,obs}$ (msec)	$T_{2'\,obs}$ (msec)	$T_{2'\,calc}$ (msec)	J (cps)	J (°K) $\times 10^{-3}$
			α-phase bcc		
22.48	80	508	0.047	1.8×10^8	8.7
22.05	62	318	0.046	1.2×10^8	5.6
21.70	45	126	0.045	4.8×10^7	2.3
21.10	29	48.0	0.044	1.9×10^7	0.93
20.12	16	17.6	0.042	7.8×10^6	0.38
			β-phase hcp		
20.12	15		0.060	3.3×10^6	0.16
19.47	7.5		0.058	1.8×10^6	0.085
19.32	8.2		0.058	2.0×10^6	0.094
18.82	3.5		0.056	8.8×10^5	0.042
18.52	2.6		0.055	6.8×10^5	0.032
18.36	2.0		0.055	5.3×10^5	0.025

[38] R. L. Garwin and A. Landesman, *Proceedings of the Eighth International Conference on Low-Temperature Physics, London, 1962* (to be published). This relaxation time has been identified to be T_{EL} and is presumably the cause of the large discrepancies in J between the present work and those given in reference 3.

[39] I. J. Lowe and R. E. Norberg, Phys. Rev. **107**, 46 (1957).

and T_2' are identical in the β phase because of the large value of T_1. A source of error at the low densities, particularly, is the fact that T_2 is not much smaller than the temperature-independent value of T_1, and hence T_2' is derived from the subtraction of two almost equal quantities.

From the calculated values of J, we see that in the low-density region of the α phase, at least, $H_{ex} \gg H_0$. This is one of the conditions for "10/3" broadening to be applicable, and, consequently, the values of J may here be too small by a factor 10/3. At the higher densities, though, $H_{ex} \leqq H_0$, so that the 10/3 effect gradually disappears. No corrections have been applied to J on this account. In the β phase, $H_{ex} \leqq H_0$, so that no 10/3 correction is here applicable. We note that J is not a monotonic function of V in the β phase, as the values for $V=19.47$ and 19.32 cm³/mole appear reversed. The apparently attractive explanation, that the densities were in fact reversed, is ruled out by examination of the T_1 data in the α phase for the same two runs, which shows that the densities are properly ordered. Both the T_1 and T_2 data show an anomaly, due presumably to nonmonotonic behavior of J. The reason for this behavior is not established.

We may compare the value of T_2' at $V=20.12$ cm³/mole here obtained at $H_0=1.6$ kG with the value obtained by GF at 9.4 kG and the same volume in the α phase. Their smallest value is twice as large as ours, but this may be due to their not extending the temperature range to low enough values. In addition, T_2' may be different for the two experiments because of the 10/3 effect, which predicts that at lower fields T_2' becomes smaller.

The α-β Phase Transition

The location of the α-β phase transition on the V-T plane may be deduced from the temperature at which discontinuities appear in the T_1 and T_2 data for various isopycnals. The results of such an investigation are shown in Table III and plotted on Fig. 2. At the molar volume 21.10 cm³/mole, the available temperature resulted only in a mixture of α and β phases, which appeared as a nonexponential T_1 recovery. At the same density and temperature, T_2 did not show any peculiar behavior in the mixed phase. This could be due to two effects: (a) T_2 is not much different in the α and β phases, or (b) only the longest T_2 is seen, due to the possibily small admixture of β phase. For these reasons, the point at $V=21.10$ is considered less well established than the rest.

TABLE III. He³ α-β phase boundaries for several different molar volumes, as determined from T_1 and T_2 relaxation times.

T, °K phase	T, °K phase
21.10 cm³/mole	19.75 cm³/mole
(T_1 only)	1.24 α
0.46 $\alpha+\beta$	1.70 α
0.51 $\alpha+\beta$	
0.562 $\alpha+\beta$	19.47 cm³/mole
0.635 α	2.105 β
	2.24 $\alpha+\beta$
20.12 cm³/mole	2.41 α
0.534 β	
0.562 $\alpha+\beta$	19.32 cm³/mole
0.597 $\alpha+\beta$	2.19 β
0.635 $\alpha+\beta$	2.26 $\alpha+\beta$
0.674 α	2.38 α

The close equality of T_2 in the two phases has been observed, for example, at $V=20.12$ cm³/mole, going from 16 to 15 msec as the phase transition is crossed. The change in T_2 upon crossing the α-β line increases rapidly as the density increases, and, extrapolating to low densities, it is not unlikely that the change in T_2 at $V=20.12$ is extremely small.

Adams, Meyer, and Fairbank[3] have conjectured that the α-β phase transition may bend sharply toward the melting line. As can be seen from Fig. 2, this conjecture is confirmed. We may also use this phase diagram to explain one of the qualitative features of the susceptibility vs temperature curves observed in reference 3. There it was observed that the curves of susceptibility vs $1/T$ fell into two groups: One which lies always below the Curie law value, and the other (at higher pressures) which went above the Curie law value before becoming constant. The latter curves were taken at pressures of 81.6, 95.3, and 112.2 atm. From our experience, the procedure there used, of slowly cooling through the solidification temperature, most likely leads to solidification at constant pressure, resulting in corresponding molar volumes of 20.86, 20.27, and 19.72 cm³/mole, respectively. From the phase diagram it is seen that at the temperature of $\sim$0.3°K these points are well within the β phase, while the ones at lower pressure are in the α phase.

Even if the solidification proceeded at constant volume, i.e., the capillary plugged immediately upon passing the freezing temperature, the two highest densities would certainly be in the β phase, while that at 81.6 might perhaps be in the β phase.

Susceptibility

Since the least-squares solution for the relaxation time T_1 also gives as an incidental parameter the value of M_0 at infinite time, as can be seen from Eq. (2), it becomes possible to determine accurately the relative molar susceptibility, provided the receiver gain is also known. A plot of echo height at infinite time, normalized to unity, and corrected for variation of T_2 with temperature, and extending from the liquid into the α, and thence the β phases, is shown in Fig. 11. This was measured at a frequency of 5.224 Mc/sec. It is seen that χ is approximately constant to within $\sim$10% across the solid-liquid phase transition, and across the α-β phase transition. At the lowest temperature there appears to be a small decrease of χ, but this is believed to be within experimental error. A run was also taken in the liquid

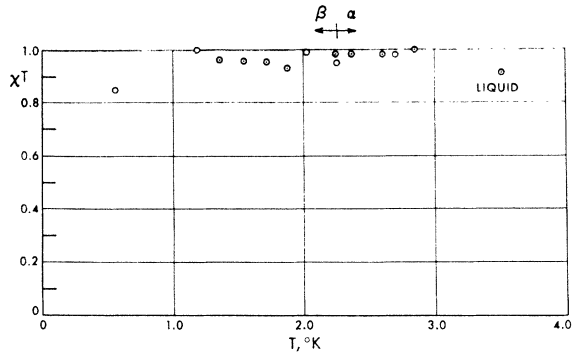

FIG. 11. χT vs T, showing that Curie's law is obeyed in both the α and β phases. The data are arbitrarily normalized to unity for the largest value of χT.

as a function of pressure, at constant temperature. Again, within experimental accuracy, the echo height was proportional to density.

Summary

By means of the spin-echo technique, direct measurements of self-diffusion, and spin relaxation times T_1 and T_2 have been made in solid He^3 at high temperatures. D shows behavior typical of vacancy diffusion at temperatures in the α phase near the melting point. As the temperature is lowered, however, D becomes constant, independent of temperature. This behavior is characteristic of quantum tunneling, and the characteristic frequency associated with the tunneling is experimentally identified as the exchange frequency J/h. The activation energy for diffusion here determined agrees quite well with that determined from specific-heat measurements. Absolute values of D are predicted well by classical considerations based on the Debye model.

At high magnetic fields, T_1 and T_2 display behavior typical of diffusion-caused relaxation, showing reasonable agreement with BPP theory advanced for liquids. At low magnetic fields and low temperatures, T_1 becomes temperature independent and depends on the magnetic field as $\exp(H^2/2H_{ex}^2)$. The transition region between relaxation to the exchange bath and relaxation to the lattice is experimentally examined in detail, and a theory developed by Hartmann is used to derive the value of the exchange integral from the temperature and field dependence of T_1.

The theory of exchange narrowing developed by Anderson and Weiss is used to deduce the value of J from observations on temperature-independent T_2. The three methods used to evaluate J show reasonable internal agreement but disagree strongly with values of J deduced from susceptibility measurements at low temperatures.

All the observations made are consistent with an exchange-lattice relaxation time of the order of T_2.

ACKNOWLEDGMENTS

The hospitality of the University of California, Berkeley, and especially of Professor E. L. Hahn, during the writing of this paper is acknowledged. We wish to thank Miss A. Willner and A. Patlach for their invaluable assistance in the experimental work. We also wish to thank Professor N. Bloembergen and Dr. S. R. Hartmann for stimulating conversations. We are grateful to Dr. Garwin and Dr. Landesman for permission to use the results of some of their experiments prior to publication.